

# Distance-Dependent Modifiable Threshold for Action Potential Back-Propagation in Hippocampal Dendrites

C. Bernard and D. Johnston

*Division of Neuroscience, Baylor College of Medicine, Houston, Texas 77030*

Submitted 24 March 2003; accepted in final form 6 May 2003

**Bernard, C. and D. Johnston.** Distance-dependent modifiable threshold for action potential back-propagation in hippocampal dendrites. *J Neurophysiol* 90: 1807–1816, 2003; 10.1152/jn.00286.2003. In hippocampal CA1 pyramidal neurons, action potentials generated in the axon back-propagate in a decremental fashion into the dendritic tree where they affect synaptic integration and synaptic plasticity. The amplitude of back-propagating action potentials (b-APs) is controlled by various biological factors, including membrane potential ( $V_m$ ). We report that, at any dendritic location ( $x$ ), the transition from weak (small-amplitude b-APs) to strong (large-amplitude b-APs) back-propagation occurs when  $V_m$  crosses a threshold potential,  $\theta_x$ . When  $V_m > \theta_x$ , back-propagation is strong (mostly active). Conversely, when  $V_m < \theta_x$ , back-propagation is weak (mostly passive).  $\theta_x$  varies linearly with the distance ( $x$ ) from the soma. Close to the soma,  $\theta_x \ll$  resting membrane potential (RMP) and a strong hyperpolarization of the membrane is necessary to switch back-propagation from strong to weak. In the distal dendrites,  $\theta_x \gg$  RMP and a strong depolarization is necessary to switch back-propagation from weak to strong. At  $\sim 260 \mu\text{m}$  from the soma,  $\theta_{260} \approx$  RMP, suggesting that in this dendritic region back-propagation starts to switch from strong to weak.  $\theta_x$  depends on the availability or state of  $\text{Na}^+$  and  $\text{K}^+$  channels. Partial blockade or phosphorylation of  $\text{K}^+$  channels decreases  $\theta_x$  and thereby increases the portion of the dendritic tree experiencing strong back-propagation. Partial blockade or inactivation of  $\text{Na}^+$  channels has the opposite effect. We conclude that  $\theta_x$  is a parameter that captures the onset of the transition from weak to strong back-propagation. Its modification may alter dendritic function under physiological and pathological conditions by changing how far large action potentials back-propagate in the dendritic tree.

## INTRODUCTION

In most mammalian central neurons, action potentials are generated in the axon region and then back-propagate into the dendritic tree (Colbert and Johnston 1996; Johnston et al. 2000; Magee et al. 1998; Spruston et al. 1995; Stuart et al. 1997). Back-propagation can be fully regenerative, decremental, or passive according to the geometrical features of the dendritic tree and the ratio between  $\text{Na}^+$  and  $\text{K}^+$  channels at any dendritic location—a property that appears to be neuron type-dependent (Hoffman et al. 1997; Martina et al. 2000; Stuart and Hausser 1994, 2001; Vetter et al. 2001).

In CA1 pyramidal neurons, the amplitude of back-propagating action potentials (b-APs) decreases with the distance from the soma due to the increase in density of  $\text{K}^+$  channels and despite a relatively uniform density of  $\text{Na}^+$  channels (Hoffman

et al. 1997; Johnston et al. 2000; Magee et al. 1998; Yuan et al. 2002). The amplitude of a b-AP at a given dendritic location is not constant either in vitro or in vivo (Quirk et al. 2001). Many factors controlling back-propagation have been described in detail (Johnston et al. 1999)—among them is the local membrane potential. Small-amplitude b-APs in the distal dendrites can be boosted by precisely timed excitatory postsynaptic potentials or appropriate membrane depolarization via A-type  $\text{K}^+$  channel inactivation and/or  $\text{Na}^+$  channel activation (Magee and Johnston 1997; Stuart and Hausser 2001). This amplification may allow the opening of voltage-gated channels and the removal of the  $\text{Mg}^{2+}$  block of NMDA receptors, hence modifying subsequent synaptic integration and providing an associative signal for synaptic plasticity (Magee and Johnston 1997; Watanabe et al. 2002). Conversely, the amplitude of b-APs can be decreased after membrane hyperpolarization (Tsubokawa and Ross 1996) or during repetitive firing of action potentials (Colbert et al. 1997). Back-propagation is thus context-specific: it depends on the availability or state (i.e., open, closed, inactivated) of  $\text{Na}^+$  and  $\text{K}^+$  channels, and the recent history of membrane potential will modify the availability (states) of these channels.

The relationship between the state of the membrane potential and the amplitude of b-APs has not been fully explored. We have investigated this issue in CA1 pyramidal neuron dendrites. We have identified two states of back-propagation, weak (small-amplitude b-AP) and strong (large-amplitude b-AP), according to the membrane potential at any given dendritic location. The transition threshold between the two states can be modified by changing the availability of  $\text{Na}^+/\text{K}^+$  channels. The possibility to switch from weak to strong or from strong to weak back-propagation provides an efficient means of modifying information processing in the dendrites.

## METHODS

Recordings were performed from CA1 pyramidal cell dendrites (Yuan et al. 2002) in 350- $\mu\text{m}$ -thick transverse hippocampal slices from male Sprague Dawley (5- to 7-wk old) according to local regulations. During recordings, slices were perfused with an oxygenated bath solution containing (in mM) 125 NaCl, 2.5 KCl, 2  $\text{CaCl}_2$ , 2  $\text{MgCl}_2$ , 1.25  $\text{NaH}_2\text{PO}_4$ , 25  $\text{NaHCO}_3$ , and 10 dextrose, kept at 32–33°C (this particular temperature was chosen to be consistent with another study in progress). 1,2,3,4-tetrahydro-6-nitro-2,3-dioxo-ben-

Present address and address for reprint requests: C. Bernard, INMED – INSERM U29, Parc Scientifique de Luminy, 13273 Marseille Cedex 09, France (E-mail: cbernard@inmed.univ-mrs.fr).

The costs of publication of this article were defrayed in part by the payment of page charges. The article must therefore be hereby marked “advertisement” in accordance with 18 U.S.C. Section 1734 solely to indicate this fact.

zof[quinoxaline-7-sulfonamide (NBQX) (1  $\mu$ M), 2-amino-5-phosphonovaleric acid (APV, 100  $\mu$ M), and bicuculline (10  $\mu$ M)/picrotoxin (10  $\mu$ M) were added to the perfusing solution to block AMPA, N-methyl-D-aspartate (NMDA) and GABA<sub>A</sub> receptors, respectively. U0126 and phorbol diacetate (PDA) were dissolved in DMSO to 10 mM. In some experiments, TTX (10  $\mu$ M) was applied near the recording microelectrode (5  $\mu$ m) using a puffer pipette (1–2  $\mu$ m tip).

Whole cell current-clamp recordings (Yuan et al. 2002) were performed using an Axoclamp 2A amplifier in bridge mode (Axon Instruments, Foster City, CA) with pipettes filled with a solution containing (in mM) 120 KMeSO<sub>4</sub>, 20 KCl, 0.2 EGTA, 2 MgCl<sub>2</sub>, 10 HEPES, 4 Na<sub>2</sub>ATP, 0.3 Tris GTP, 14 phosphocreatine; 0.4% biocytin and KOH were added to adjust to pH 7.3. Stimulation and data acquisition were controlled by Igor software (Igor Wavemetrics). Signals were digitized with an ITC-18 interface (Instrutech), at a sampling rate of 5–20 kHz. Access resistance as estimated from the bridge balance was  $33.9 \pm 1.3$  (SE) M $\Omega$  ( $n = 65$ ). Experiments for which access resistance increased by >20% or went over 50 M $\Omega$  were discarded. Input resistance was  $102 \pm 4$  M $\Omega$ , as measured from 5-ms-duration current steps ( $n = 65$ ) (see Durand et al. 1983). Antidromic action potentials were evoked every 20 s by 0.1-ms constant current pulses through tungsten electrodes placed at the alveus/stratum oriens border. PDA induced a depolarization of the resting membrane potential by 15–20 mV as reported before (Yuan et al. 2002). This depolarization was compensated by current injection.

Slices were processed for morphology, and all 65 neurons were morphologically identified as CA1 pyramidal cells post hoc (Cossart et al. 2000). The distance between the recording site in the dendrite and the soma (start of the main apical dendritic trunk) was first evaluated on-line using the projected infrared image on the video screen and confirmed morphologically post hoc, the recording site appearing as a hole or a dent in the dendritic tree (Cossart et al. 2000).

Significance ( $P < 0.05$ ) was determined by two-sample  $t$ -test. Error bars represent SE.

## RESULTS

### b-AP amplitude and membrane potential

Antidromic action potentials were evoked by extracellular stimulation at the alveus/stratum oriens border. b-AP amplitude decreased with the distance from the soma at resting membrane potential (Fig. 1A), consistent with previous studies (Golding et al. 2001; Hoffman et al. 1997; Spruston et al. 1995;

Yuan et al. 2002). The decrease in amplitude of b-APs was correlated to the decrease of the maximal rate of rise of the b-APs (Fig. 1, B and C). The half-width of the b-APs increased with the distance from the soma (Fig. 1D).

Current pulses were injected into the dendrites in a step-wise manner to achieve various membrane potentials ( $V_m$ ), from hyperpolarized (–120 to –90 mV) to depolarized (subthreshold to action potential initiation) levels. b-APs were evoked 300 ms after the start of current injection to allow membrane potential to reach steady state. Figure 2 illustrates the results obtained with such a protocol (dendrite recorded 260  $\mu$ m from the soma). The amplitude of b-APs remained small and roughly constant over a wide range of hyperpolarized potentials (Fig. 2, A and B). As the membrane was further depolarized, there was a rapid increase of the relative amplitude of b-APs until it decreased because the membrane potential at the peak of the b-AP reached an asymptotic value (Fig. 2C). The maximum rate of rise of the b-APs followed the same type of curve (not shown). The half-width of the b-APs was large at hyperpolarized levels and decreased as  $V_m$  became more positive till it reached a minimum (Fig. 2D). The half-width then increased as the membrane was further depolarized. The broadening of b-APs at depolarized levels might reflect the activation of voltage-gated Ca<sup>2+</sup> channels.

We define  $\theta$  as the membrane potential where the second derivative of the b-AP amplitude (Amp) with respect to  $V_m$  is maximum, i.e.,  $\theta = \max[d^2\text{Amp}(V_m)/dV_m^2]$  (Fig. 2E).  $\theta$  represents the onset of the transition between small- and large-amplitude (weak and strong) back-propagation. In the example shown in Fig. 2, the resting membrane potential (RMP) of the dendrite was –68 mV and  $\theta$  was –58 mV. In this dendrite, at 260  $\mu$ m from the soma, b-APs had a small amplitude because RMP was more negative than  $\theta$  (RMP <  $\theta$ ). For boosting or amplification to occur,  $V_m$  had to reach  $\theta = -58$  mV.

Rapid changes in membrane potential occur in vivo, in particular during oscillations (Buzsáki 2002). Sinusoidal currents were injected in the dendrites at various frequencies, and b-APs were appropriately timed to mimic physiologically relevant conditions (Stuart and Hausser 2001). b-APs displayed a transition from weak to strong (or from strong to weak) back-

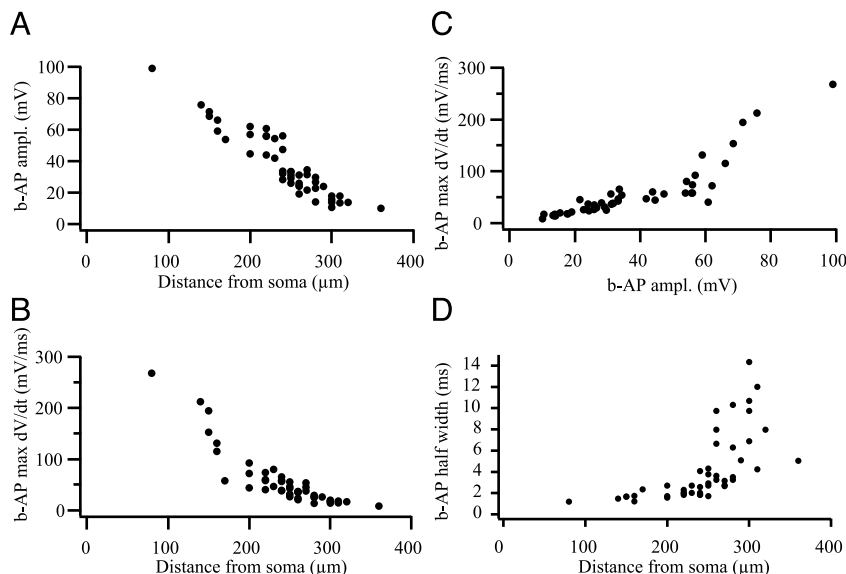
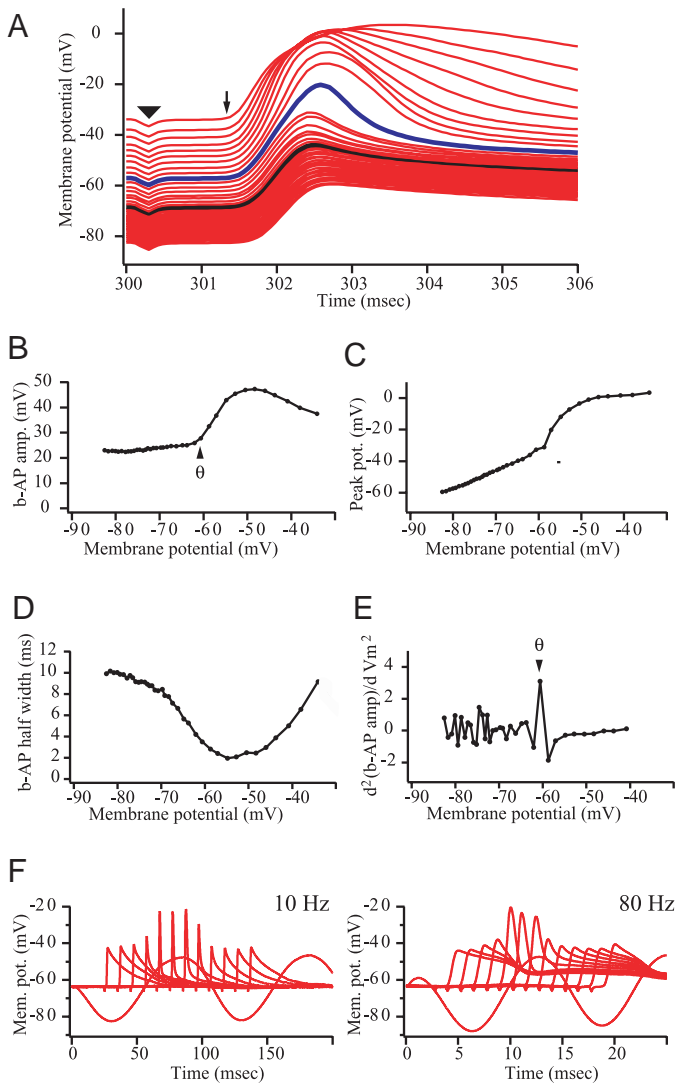


FIG. 1. Back-propagating action potentials in CA1 pyramidal cell dendrites ( $n = 65$  recordings). A: the amplitude of the back-propagating action potential (b-AP) decreased progressively as a function of the distance from the soma. B: the maximal rate of rise (given by the maximum of the derivative of the rising phase of the action potential) also decreased progressively with the distance from the soma. C: maximal rate of rise as a function of b-AP amplitude measured at resting membrane potential. For b-AP of <60 mV amplitude, the relationship between the 2 variables was linear and the slope is 1. D: the half-width of the b-AP increased with the distance from the soma.



**FIG. 2.** Transition threshold ( $\theta$ ) between weak and strong back-propagation of action potentials. Example of a dendrite recorded  $260 \mu\text{m}$  from the soma. **A:** the amplitude of the b-AP varied with membrane potential. Note the sudden increase in amplitude as the membrane was depolarized (blue trace). Black trace: b-AP at resting membrane potential at the dendritic recording site. Note that the peak amplitude of the b-AP reached a maximum value as the membrane approached depolarized levels of around  $-40 \text{ mV}$ . Arrowhead: stimulus artifact. Small arrow: foot of b-AP. **B:** the variation of b-AP amplitude followed a sigmoid-like curve. The amplitude of the b-AP remained constant in the hyperpolarized range, there was then a rapid increase until the amplitude reached a maximum value before decreasing. Arrowhead indicates  $\theta$  the threshold for the transition between small and large amplitude b-APs ( $\theta$  is the membrane potential where the second derivative of the sigmoid with respect to  $V_m$  is maximum). **C:** the membrane potential at the peak of the action potential increased linearly with the depolarization, sharply above  $\theta$ , then stabilized at a maximum value. This maximum value explains why the b-AP amplitude started to decrease at around  $-40 \text{ mV}$  in **B**. **D:** the half-width of the b-AP decreased with membrane depolarization as more and more  $\text{K}^+$  channels become available till it starts to increase again probably because of the activation of  $\text{Ca}^{2+}$  channels. **E:** the membrane potential for which the 2nd derivative of the amplitude of b-AP with respect to  $V_m$  is maximum gives the value of the transition threshold,  $\theta$ . **F:** the transition between small- and large-amplitude back-propagation occurred on sinusoidal variation of membrane potential mimicking oscillations at 10 Hz (left) and 80 Hz (right). The graphs show the variation of membrane potential during the current injection in the absence of b-AP. b-APs were then triggered at different times during the oscillation. The curves thus obtained were subtracted from the curve with no b-AP and superimposed on the graph. Transitions between small (large)- and large (small)-amplitude back-propagation occurred on reaching the peak (trough) of the oscillation.

propagation similar to that obtained with constant dendritic current injection ( $n = 50$ , Fig. 2F), showing that transitions can occur on a very fast time scale.

*From strong to weak back-propagation*

A transition threshold was found in 62 of the 65 recorded dendrites. In three cases (distal recordings  $>300 \mu\text{m}$ ), the transition could not be identified because action potentials were triggered by the current injection before the occurrence of the b-AP. The value of  $\theta$  varied linearly along the dendritic tree, increasing with distance ( $x$ ) from the soma (Fig. 3A), from hyperpolarized values (with respect to RMP) for distances close to the soma to depolarized values in the distal part of the dendritic tree. By subtracting  $\theta_x$  from RMP at each recording site, we found two main regions of back-propagation along the dendritic tree (Fig. 3B). Below the zero line, RMP was more positive than  $\theta_x$  and b-APs had a large amplitude (strong back-propagation). Membrane hyperpolarization could switch back-propagation from strong to weak, provided that  $V_m < \theta_x$ . Above the zero line, RMP was more negative than  $\theta_x$ , and b-APs had a small amplitude (weak back-propagation). Membrane depolarization switched back-propagation from weak to strong, provided that  $V_m > \theta_x$ . Therefore the critical factor that determined whether strong or weak back-propagation occurred was where  $V_m$  was with respect to  $\theta_x$  at any dendritic location ( $x$ ). The intersection between the zero line and the regression line of  $\theta_x$  gave the average distance from the soma in the

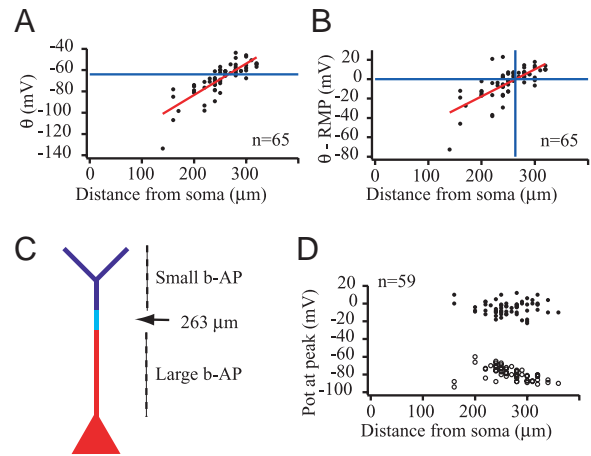


**FIG. 3.** From strong to weak back-propagation in dendritic trees. **A:** the threshold for amplification increased as a function of the distance from the soma. The blue line represents the average RMP in the dendrite of the 65 recordings. The red line is the linear least-square best fit of the dataset. **B:** difference between the transition threshold and RMP at each recording site as a function of the distance from the soma. Above (below) the blue line, where  $\text{RMP} = \theta$ , b-APs had a small (large) amplitude. The intersect between the blue line and the linear least-square best fit of the dataset gives the distance in the dendritic tree where, on average,  $\text{RMP} = \theta$ , i.e.,  $263 \mu\text{m}$  from the soma. **C:** we propose the following model:  $<263 \mu\text{m}$ , b-APs have a large amplitude because  $\text{RMP} > \theta$  (red portion of the dendritic tree). In the intermediate zone around  $263 \mu\text{m}$ , the amplitude of the b-AP decreases sharply (light blue). The extent of the light blue zone (extent of the transition zone) is arbitrary as it varied from cell to cell. At distances more than  $263 \mu\text{m}$ , b-APs have a small amplitude because  $\text{RMP} < \theta$  (dark blue portion of the dendritic tree). **D:** the maximum depolarization reached at the peak of the b-AP was roughly constant along the dendritic tree when the membrane was held at  $-35 \text{ mV}$  (●) or at  $-100 \text{ mV}$  (○). The dynamic range of the membrane depolarization achieved by b-APs was constant along the portion of the dendritic tree tested with these two holding potentials as limits.

dendritic tree where  $RMP = \theta_x$ . We found a value of  $x = 263 \pm 6 \mu\text{m}$ .

$\theta_x$  captures the onset of the transition between weak and strong back-propagation. We define the length of the transition zone as the interval between  $\theta_x$  and the membrane potential corresponding to the end of the rising phase of  $\text{Amp}(V_m)$ . In Fig. 2B,  $\theta_x = -58 \text{ mV}$ , the end of the rising phase was at  $-49 \text{ mV}$ , which gave a length for the transition zone of  $9 \text{ mV}$ . There was no obvious relationship between the length of the transition zone and the distance from the soma, although the general trend was an increase of the length of the transition zone with the distance from the soma (not shown). In Fig. 8C, the recording site was at  $280 \mu\text{m}$ , and the transition length was  $4 \text{ mV}$  [ $\text{Amp}(V_m)$  was more like a step function], shorter than the  $9 \text{ mV}$  measured  $260 \mu\text{m}$  from the soma in Fig. 2.

We propose the following scheme (Fig. 3C). When an action potential is generated in the axon, it back-propagates into the dendritic tree. Its amplitude decreases with the distance from the soma as the density of A-type  $\text{K}^+$  channels increases. Between the soma and  $263 \mu\text{m}$ , the b-AP amplitude remains large because  $RMP > \theta_x$ . Before reaching  $263 \mu\text{m}$ , there is a sudden acceleration of the decrease of amplitude (falling phase of  $\text{Amp}(V_m)$ ). At distances more than  $263 \mu\text{m}$ , the b-AP has a small amplitude because  $RMP < \theta_x$ , and its amplitude still decreases with distance from the soma. Consistent with this scheme, most recordings performed at distances  $< 263$  and  $> 263 \mu\text{m}$  displayed large and small b-APs, respectively (Fig. 3B).

The amplitude of b-APs is a critical parameter to consider for  $\text{Ca}^{2+}$  signaling in dendrites (Magee et al. 1998). We thus determined the dynamic range of membrane potentials generated by b-APs along the dendritic tree. For a measured (or extrapolated)  $V_m$  of  $-100 \text{ mV}$ , b-APs had a small amplitude because  $V_m \ll \theta_x$  (weak back-propagation). The amplitude of the b-APs was remarkably constant at this potential at all recording sites ( $21 \pm 1 \text{ mV}$ ,  $n = 59$ ). For a holding potential of  $-100 \text{ mV}$ , the membrane potential reached at the peak by b-APs was thus  $-79 \pm 1 \text{ mV}$ ,  $n = 59$ , Fig. 3D. The amplitude of the b-APs for a holding potential of  $-35 \text{ mV}$  was also remarkably constant along the dendritic tree ( $30 \pm 1 \text{ mV}$ ,  $n = 59$ ). At this holding potential,  $V_m \gg \theta_x$  (strong back-propagation). For a holding potential of  $-35 \text{ mV}$ , the membrane potential reached at the peak by b-APs was thus  $-5 \pm 1 \text{ mV}$ ,  $n = 59$ , Fig. 3D. If we consider  $-100$  and  $-35 \text{ mV}$  as lower and upper limits for membrane potential fluctuations, respectively, the membrane potential reached at the peak of b-APs can evolve between location-independent lower ( $-79 \text{ mV}$ ) and upper ( $-5 \text{ mV}$ ) boundaries with a wide dynamic range ( $-75 \pm 2 \text{ mV}$ ,  $n = 59$ ).

In the distal part of the dendritic tree, b-APs may not open sufficient numbers of  $\text{Na}^+$  channels to be actively propagated. To test this, we selected dendritic recordings for which  $RMP$  was less than  $\theta$  (weak back-propagation) and for which the amplitude of the b-AP was between  $20$  and  $30 \text{ mV}$  at  $RMP$ . Local application of the  $\text{Na}^+$  channel blocker TTX ( $10 \mu\text{M}$ ) had no effect on the amplitude of b-APs ( $n = 3$ , Fig. 4A), consistent with a passive back-propagation. This lack of effect was not due to a failure of TTX ejection as moving the puff pipette closer to the soma on the same dendrites ( $200 \mu\text{m}$ ) slightly reduced the amplitude of b-APs recorded more distally ( $n = 3$ , not shown). We also selected dendritic recordings for

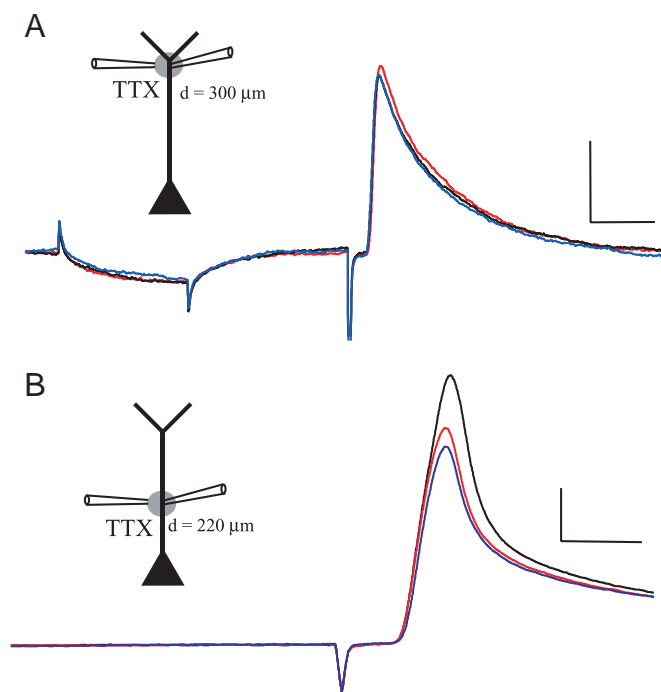


FIG. 4. Weak back-propagating action potentials failed to open  $\text{Na}^+$  channels. *A*: local application ( $5 \mu\text{m}$  away from the recording electrode) of the  $\text{Na}^+$  channel blocker TTX ( $10 \mu\text{M}$  in puff pipette) did not modify the amplitude of the b-AP. Black trace (before TTX) as well as red and blue traces (after TTX at 2 different pressures) are superimposed. Example of a dendrite recorded  $300 \mu\text{m}$  from the soma. Scale bar  $5 \text{ mV}/10 \text{ ms}$ . *B*: in contrast, TTX (at 2 different pressures as above) produced a decrease in b-AP amplitude for recordings performed closer to the soma ( $220 \mu\text{m}$  in this example). Scale bar  $5 \text{ mV}/2.5 \text{ ms}$ .

which  $RMP$  was over  $\theta$  (strong back-propagation) and for which the amplitude of the b-AP was between  $40$  and  $50 \text{ mV}$ . Local application of TTX decreased the amplitude of b-APs ( $n = 3$ , Fig. 4B), consistent with a back-propagation containing an active component. Interestingly, the basic features of b-APs evoked at  $V_m < \theta_x$  at any dendritic location ( $x$ ) were identical to those measured at  $RMP$  at a distance  $> 270 \mu\text{m}$  from the soma; i.e., amplitude ( $20$ – $30 \text{ mV}$ ), maximum rate of rise ( $20$ – $30 \text{ mV/ms}$ ) and half-width ( $3$ – $15 \text{ ms}$ ). This suggests that at potentials less than  $\theta_x$ , back-propagation is mostly passive, and we propose that  $\theta_x$  corresponds to the potential where the transition from a back-propagation containing an active component to a passive one occurs.

#### $\theta$ and $\text{Na}^+/\text{K}^+$ channel availability

The amplitude of b-APs appears to be controlled by the degree of activation/inactivation as well as by the density of  $\text{Na}^+$  and  $\text{K}^+$  channels (Pan and Colbert 2001). We investigated the consequences of slight modifications of  $\text{Na}/\text{K}$  channel availability on the transition threshold  $\theta$ .

Partial blockade of  $\text{Na}^+$  channels with  $10 \text{ nM}$  TTX decreased the amplitude of b-APs to  $61 \pm 10\%$  of control at  $RMP$  ( $n = 6$ ,  $P < 0.02$ ) and shifted  $\theta$  by  $10 \pm 4 \text{ mV}$  ( $n = 6$ ,  $P < 0.03$ ) toward depolarized values (Fig. 5A). The distance in the dendritic tree where  $RMP$  was close to the new threshold with  $10 \text{ nM}$  TTX was now  $254 \pm 30 \mu\text{m}$  from the soma.

Partial blockade of  $\text{K}^+$  channels with  $50 \mu\text{M}$  4-aminopyridine (4-AP) (Hoffman et al. 1997) produced a small but not

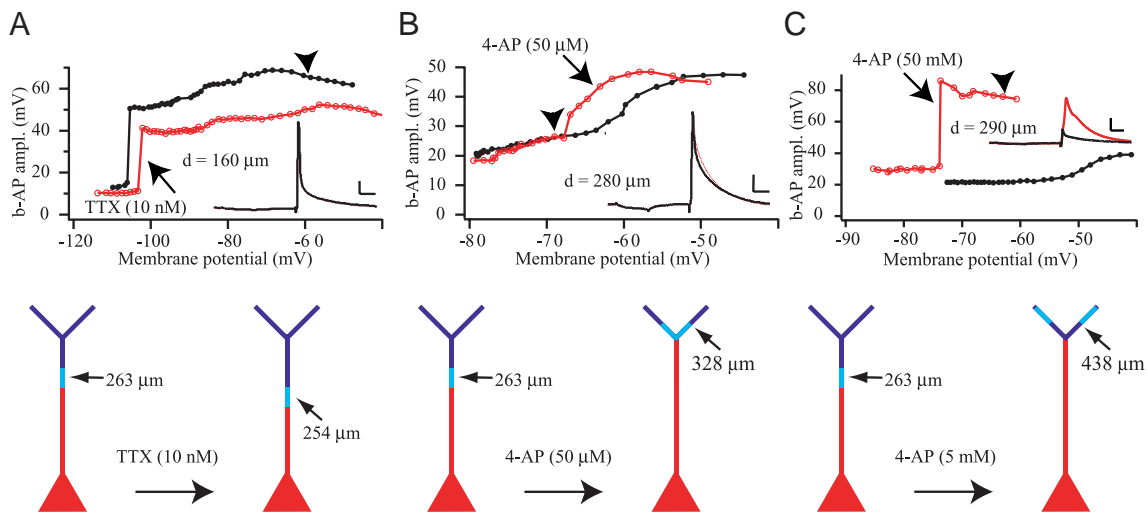


FIG. 5. Modification of  $\theta$  after partial blockade of  $\text{Na}^+$  and  $\text{K}^+$  channels. **A**: application of a small dose of the  $\text{Na}^+$  channel blocker TTX (10 nM) shifted the transition threshold to a more positive value. Example of a dendrite recorded 160  $\mu\text{m}$  from the soma. *Top*: variation of b-AP amplitude as a function of membrane potential before (filled black circles) and after TTX (empty red circles). Amp( $V_m$ ), here a step-like function, and  $\theta$  were shifted to the right. The amplitude of b-APs was smaller at all membrane potentials, including at RMP ( $-60$  mV, arrowhead) because of the partial blockade of  $\text{Na}^+$  channels. *Inset*: b-AP before (black) and after (red) TTX at RMP. Traces are superimposed, because the decrease in amplitude was small. Scale bar: 10 mV/10 ms. *Bottom*: the shift to the right of  $\theta$  resulted in a shift toward the soma of the portion of the apical dendrite that had b-APs with a large amplitude, from 263 to 254  $\mu\text{m}$ . **B**: application of the  $\text{K}^+$  channel blocker 4-AP (50  $\mu\text{M}$ ) shifted the transition threshold to a more negative value. Example of a dendrite recorded 280  $\mu\text{m}$  from the soma. *Top*: variation of b-AP amplitude as a function of membrane potential before (filled black circles) and after 4-AP (empty red circles). Amp( $V_m$ ), here a smooth sigmoid-like function, and  $\theta$  were shifted to the left. In this example, the amplitude of b-APs was increased in the rising phase of the sigmoid-like function after 4-AP. The minimum and maximum amplitudes of b-APs were similar before and after 4-AP. *Inset*: b-AP before (black) and after (red) 4-AP at RMP ( $-68$  mV). Traces superimpose, because b-AP amplitudes were identical at RMP (arrowhead). The effect of partial blockade of  $\text{K}^+$  channel was apparent as an increase of the repolarization phase of the b-AP after 4-AP. Scale bar: 5 mV/10 ms. *Bottom*: the shift to the left of  $\theta$  resulted in a shift toward the distal portion of the apical dendrite that sees b-APs with a large amplitude, from 263 to 328  $\mu\text{m}$ . **C**: application of the  $\text{K}^+$  channel blocker 4-AP (5 mM) shifted the transition threshold to a more negative value. Example of a dendrite recorded 290  $\mu\text{m}$  from the soma. *Top*: variation of b-AP amplitude as a function of membrane potential before (filled black circles) and after 5 mM 4-AP (empty red circles). Amp( $V_m$ ), here a smooth sigmoid-like function, and  $\theta$  were shifted to the left. The minimum and maximum amplitudes of b-APs were increased after 4-AP. *Inset*: b-AP before (black) and after (red) 4-AP at RMP ( $-63$  mV). Scale bar: 20 mV/10 ms. *Bottom*: the shift to the left of  $\theta$  resulted in a shift toward the distal portion of the apical dendrite that sees b-APs with a large amplitude, from 263 to 438  $\mu\text{m}$ .

statistically significant increase of the average amplitude of b-APs ( $128 \pm 16\%$  of control at RMP;  $n = 6$ ,  $P = 0.15$ ) but significantly shifted  $\theta$  by  $7.8 \pm 3.3$  mV ( $n = 6$ ,  $P < 0.05$ ) toward hyperpolarized values (Fig. 5B). The distance in the dendritic tree where RMP was close to the new threshold with 50  $\mu\text{M}$  4AP was now  $328 \pm 49$   $\mu\text{m}$  from the soma. Larger blockade of  $\text{K}^+$  channels with 5 mM 4AP, in the presence of 0.2 mM  $\text{Cd}^{2+}$  and 0.2 mM  $\text{Ni}^{2+}$  (Hoffman et al. 1997), increased the amplitude of back-propagating action potentials to  $237 \pm 33\%$  of control at RMP ( $n = 11$ ,  $P < 0.001$ ) and shifted the threshold by  $14.8 \pm 4.4$  mV ( $n = 11$ ,  $P < 0.001$ ) toward hyperpolarized values (Fig. 5C). The distance in the dendritic tree where RMP was close to the new threshold with 5 mM 4AP was now  $438 \pm 48$   $\mu\text{m}$  from the soma.

In conclusion,  $\theta$  was modified by changing the number of  $\text{Na}^+$  and  $\text{K}^+$  channels available for activation. A decreased number of  $\text{Na}^+$  channels limited the extent of the dendritic tree where strong back-propagation occurred. Conversely, a decreased number of  $\text{K}^+$  channels led to large-amplitude b-APs invading farther into the dendritic tree.

#### $\theta$ is not $I_h$ sensitive

Hyperpolarization-activated current ( $I_h$ ) is present at high density in CA1 pyramidal neuron dendrites. Similarly to A-

type  $\text{K}^+$  channels, the density of  $I_h$  channels increases many-fold with the distance from the soma (Magee 1998). We therefore tested whether  $I_h$  played a role in controlling  $\theta$ . Application of the  $I_h$  antagonist ZD7288 (30  $\mu\text{M}$ ) slightly decreased the average amplitude of back-propagating action potentials at RMP by  $7 \pm 3\%$  of control (Fig. 6), but this decrease was not statistically significant ( $n = 5$ ,  $P = 0.06$ ). The transition threshold was also not modified (Fig. 6,  $-0.3 \pm 0.5$  mV,  $n = 5$ ,  $P = 0.3$ ). We conclude that  $I_h$  does not affect the distance from the soma where the transition from strong to weak back-propagation occurred in the apical dendrites.

#### Effect of $\text{Na}^+$ channel inactivation on $\theta$

b-APs undergo activity-dependent attenuation of their amplitude (Callaway and Ross 1995; Colbert et al. 1997; Spruston et al. 1995). During repetitive firing, there is a change in the Na/K channel ratio in favor of  $\text{K}^+$  channels, because  $\text{Na}^+$  channel inactivation increases during the train while  $\text{K}^+$  channels do not (Colbert et al. 1997; Pan and Colbert 2001). To study the consequences of  $\text{Na}^+$  channel inactivation on  $\theta$ , a train of five b-APs was generated in the dendrites with a 50-ms interstimulus interval. The amplitude of b-APs decreased in an activity-dependent manner and was seen as soon as the second b-AP in the train (Fig. 7A), consistent with previous studies

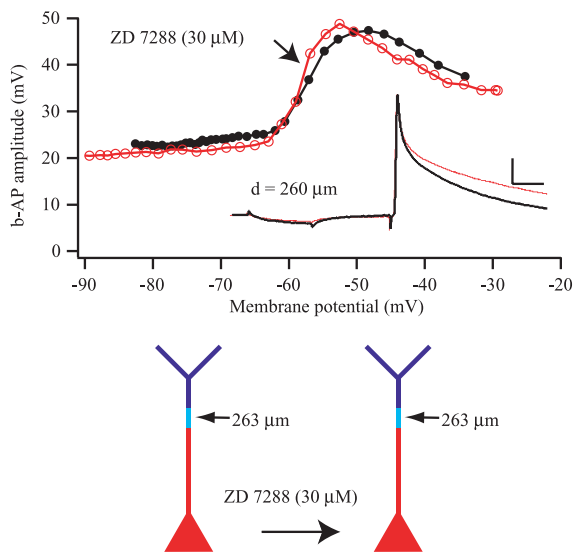


FIG. 6.  $I_h$  did not affect  $\theta$ . Example of a dendrite recorded 260  $\mu\text{m}$  from the soma (same as Fig. 2). *Top*: total blockade of  $I_h$  with ZD 7288 (30  $\mu\text{M}$ ) did not change the relationship between b-AP amplitude and membrane potential;  $\theta$  was not modified. *Inset*: b-AP before (black) and after (red) ZD 7288 at RMP ( $-64$  mV). The amplitude of the b-AP was not modified but the repolarization phase of the b-AP was increased. Scale bar: 5 mV/10 ms. *Bottom*: blocking  $I_h$  did not change back-propagation in the dendritic tree.

(Callaway and Ross 1995; Colbert et al. 1997; Spruston et al. 1995). However, this activity-dependent decrease of b-AP amplitude was also voltage-dependent (Fig. 7A). The Amp ( $V_m$ ) curves had the same shape for all b-APs in the train, each with a specific transition threshold (Fig. 7B). The transition threshold was progressively shifted to more positive membrane potentials as the inactivation of  $\text{Na}^+$  channels increased (Fig. 7B). The effect of  $\text{Na}^+$  channel inactivation was also evident on the b-AP rising phase slope, which decreased in an activity-dependent manner (Fig. 7B). The ratio between the last and the first b-AP amplitude as a function of membrane potential followed a multiphasic curve (Fig. 7C). In the example presented in Fig. 7, at potentials lower than the transition threshold for the first b-AP, the ratio decreased slowly. On reaching  $\theta_{1st}$  there was a sudden drop of the ratio because of the sudden increase in amplitude of the first b-AP while the amplitude of the last b-AP remained unchanged. On reaching  $\theta_{5th}$ , the ratio increased as the amplitude of the last b-AP increased rapidly before stabilizing (Fig. 7C).

This experimental protocol was performed in 56 dendrites at various distances from the soma. Figure 7D shows a continuous decrease in amplitude of the last b-AP in the train as a function of the distance from the soma ( $n = 56$ ). A transition threshold for the last b-AP was found in 27% of the recordings (Fig. 7E;  $n = 15/56$ ). In the remaining recordings ( $n = 41$ ), the membrane potential did not reach  $\theta_{5th}$ . However, some experimental manipulations resulted in a shift of  $\theta_{5th}$  to more negative values, such as a partial blockade of  $\text{K}^+$  channels (not shown) or their phosphorylation (Fig. 8A), allowing the transition to occur within the range of membrane potentials tested. There was no obvious correlation with the absence of  $\theta_{5th}$  and the distance to the soma or the amplitude of the first b-AP. The difference between  $\theta_{1st}$  and  $\theta_{5th}$  varied between 1.3 and 16.7 mV ( $9.1 \pm 2.3$  mV,  $n = 15$ ) and seemed to be independent of

the recording site (Fig. 7E). The distance from the soma where  $\theta_{5th} = \text{RMP}$  was found to be  $235 \pm 18$   $\mu\text{m}$  (Fig. 7, E and F).

These data indicate that the progressive inactivation of  $\text{Na}^+$  channels during high-frequency firing results in a progressive shift of the transition threshold toward more positive values. Not surprisingly, this was similar to that observed with low concentrations of TTX.

#### PKC activation favors strong back-propagation

Protein kinase A and protein kinase C (PKC) activations produce similar positive shifts in the activation curve of A-type  $\text{K}^+$  channels via the MAPK pathway. As a result, fewer  $\text{K}^+$  channels become available for opening, and the amplitude of b-APs is consequently increased (Hoffman and Johnston 1998, 1999; Yuan et al. 2002). Also, increases in PKC activity reduce slow  $\text{Na}^+$  channel inactivation resulting in less b-AP attenuation during a train (Colbert and Johnston 1998) (Fig. 8A). Such phenomena could be physiologically important given that synaptic plasticity is accompanied by both transient and persistent increases in protein kinase activity (Adams and Sweatt 2002; Colbert and Johnston 1998; English and Sweatt 1996). We thus tested the consequences of PKC activation on the transition threshold  $\theta$ . PKC activation after application of 10  $\mu\text{M}$  PDA increased the amplitude of b-APs to  $157 \pm 16\%$  of control at RMP ( $n = 6$ ,  $P < 0.02$ ) and shifted the threshold by  $17.8 \pm 5.9$  mV ( $n = 6$ ,  $P < 0.02$ ) to more negative values (Fig. 8A). The distance in the dendritic tree where RMP was close to the new threshold after PDA was now  $425 \pm 102$   $\mu\text{m}$  from the soma. Although PKC-dependent changes of  $\text{K}^+$  and  $\text{Na}^+$  activation curves should result in opposite shifts of  $\theta$  (toward more negative and positive values, respectively), the effect on  $\text{K}^+$  channels is predominant and PKC activation significantly increases the extent of the dendritic tree that sees large-amplitude b-APs.

#### Preventing phosphorylation favors weak back-propagation

An endogenous phosphorylation of A-type  $\text{K}^+$  channels has been reported in vitro (Watanabe et al. 2002; Yuan et al. 2002). Furthermore, certain properties of Na/K channels are modulated by phosphorylation in a distance-dependent manner (Gasparini and Magee 2002; Hoffman and Johnston 1998; Yuan et al. 2002), further suggesting that there may be a gradient of endogenous kinase activity along the dendrites. We thus tested the effect of the broad spectrum protein kinase inhibitor H7 on  $\theta$ . Bath application of H7 for 30 min resulted in a decrease of the amplitude of b-APs to  $88 \pm 4\%$  of control at RMP ( $n = 5$ ,  $P < 0.03$ ), in keeping with the hypothesis of an endogenous phosphorylation of Na/K channels under physiological conditions. H7 also shifted  $\theta$  by  $4.7 \pm 0.7$  mV ( $n = 5$ ,  $P < 0.002$ ) toward depolarized values (Fig. 8B). The distance in the dendritic tree where RMP was close to the new threshold with H7 was now  $243 \pm 22$   $\mu\text{m}$  from the soma.

Protein kinase A and PKC can phosphorylate Kv4.2 channels via the extracellular regulated kinase (ERK) pathway (Yuan et al. 2002). Kv4.2 channels constitute the most abundant transient  $\text{K}^+$  channels in CA1 pyramidal cells, in particular, in the dendrites where they directly control the

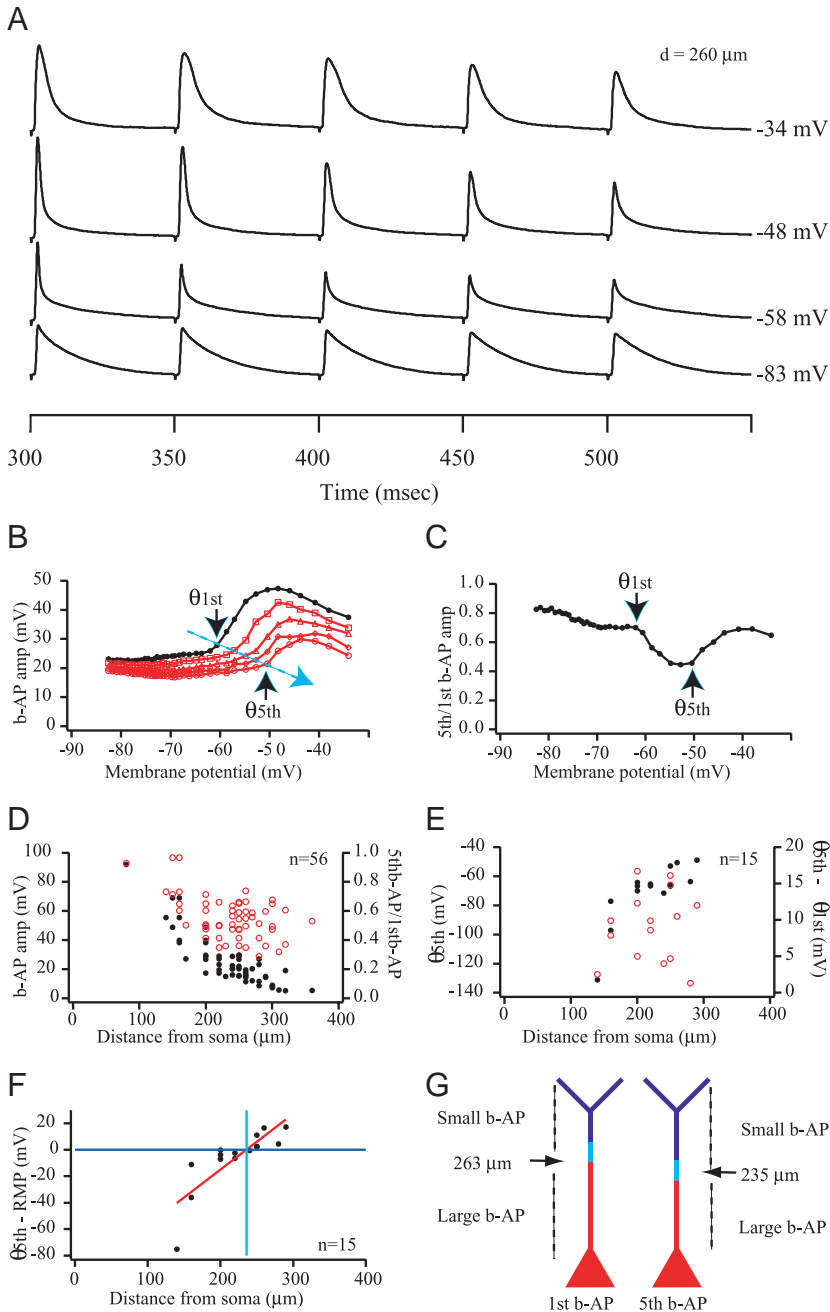


FIG. 7. Activity-dependent inactivation of Na<sup>+</sup> channels shifted  $\theta$  to more positive values. *A*: example of a dendrite recorded 260  $\mu\text{m}$  from the soma (same as Figs. 2 and 5). b-AP amplitude decreased during repetitive firing activity. b-APs in the train displayed different transition thresholds. At  $-83\text{ mV}$ , all b-APs had a small, similar amplitude. At  $-58\text{ mV}$ , the 1st b-AP became large, while the 5th remained small. At  $-48\text{ mV}$ , the 1st had a large amplitude, and the amplitude of the 5th became larger. *B*: each b-AP in the train had its own transition threshold that was shifted toward more negative values the more Na<sup>+</sup> channels inactivated (1st b-AP,  $\bullet$ ; 2nd b-AP,  $\square$ ; 3rd b-AP,  $\triangle$ ; 4th b-AP,  $\diamond$ ; 5th b-AP,  $\circ$ ). The maximum amplitude reached by b-APs decreased also as Na<sup>+</sup> channels inactivated. *C*: the ratio between the 5th and the 1st b-AP in the train followed a multiphasic curve as a function of membrane potential. If  $V_m < \theta_{1st}$ , the ratio decreased slowly and stabilized  $\sim 70\%$ . If  $\theta_{1st} < V_m < \theta_{5th}$ , there was a sudden drop of the ratio to  $\sim 40\%$  as the amplitude of the 1st b-AP sharply increased with membrane depolarization while the amplitude of the 5th b-AP remained constant. If  $V_m > \theta_{5th}$ , the amplitude of the 5th b-AP sharply increased and the ratio came back to  $\sim 70\%$ . *D*: the amplitude of the 5th b-AP decreased progressively as a function of the distance from the soma ( $\bullet$ ,  $n = 56$ ). The ratio between the 5th and 1st b-AP at RMP also displayed a general trend of decrease as the distance from the soma increased ( $\circ$ ,  $n = 56$ ). *E*: a transition threshold for the 5th b-AP in the train was found in 15 of 56 recordings. As for  $\theta_{1st}$ ,  $\theta_{5th}$  increased with the distance from the soma ( $\bullet$ ,  $n = 15$ ). There was no obvious correlation with the difference  $\theta_{5th} - \theta_{1st}$  and the distance from the soma ( $\circ$ ,  $n = 15$ ). *F*: difference between  $\theta_{5th}$  and RMP as a function of distance from the soma. Above (below) the blue line, where RMP =  $\theta_{5th}$ , the 5th b-AP had a small (large) amplitude. The intersect between the blue line and the linear least-square best fit of the dataset gave the distance in the dendritic tree where RMP =  $\theta_{5th}$ , i.e., 235  $\mu\text{m}$  from the soma. *G*: inactivation of Na<sup>+</sup> channels changed the mode of back-propagation in the dendritic tree. The transition zone was at 263  $\mu\text{m}$  for the 1st b-AP and at 235  $\mu\text{m}$  for the 5th b-AP.

amplitude of b-APs. We have thus applied the MEK inhibitor U0126 to prevent the phosphorylation of Kv4.2 channels. Bath application of U0126 for 30 min resulted in a decrease of the amplitude of b-APs to  $81 \pm 3\%$  of control at RMP ( $n = 10$ ,  $P < 0.0001$ ), in keeping with the endogenous phosphorylation of Kv4.2 channels under physiological conditions (Adams and Sweatt 2002; Yuan et al. 2002). U0126 also shifted  $\theta$  by  $5.1 \pm 1.0\text{ mV}$  ( $n = 10$ ,  $P < 0.0001$ ) toward depolarized values (Fig. 8C). The distance in the dendritic tree where RMP was close to the new threshold after U0126 application was now reduced to  $222 \pm 31\ \mu\text{m}$  from the soma.

Therefore the endogenous phosphorylation of Na<sup>+</sup> and K<sup>+</sup> channels extends the portion of the apical dendrite that sees large-amplitude b-APs.

DISCUSSION

We describe a distance-dependent threshold  $\theta_x$  that captures the onset of the transition from weak to strong or from strong to weak back-propagation in the main apical dendrite of CA1 pyramidal neurons. The transition from strong (mainly active) to weak (mainly passive) back-propagation occurs  $\sim 260\ \mu\text{m}$  from the soma at RMP. The transition from strong (weak) to weak (strong) back-propagation can also take place anywhere along the dendritic tree following appropriately timed changes in membrane potential  $V_m$ , with the direction of the transition depending on the difference between  $V_m$  and  $\theta_x$ .  $\theta_x$  reflects the availability of ionic channels at any dendritic location, in particular Na<sup>+</sup>/K<sup>+</sup> channels, and can be dynamically modified. A change in

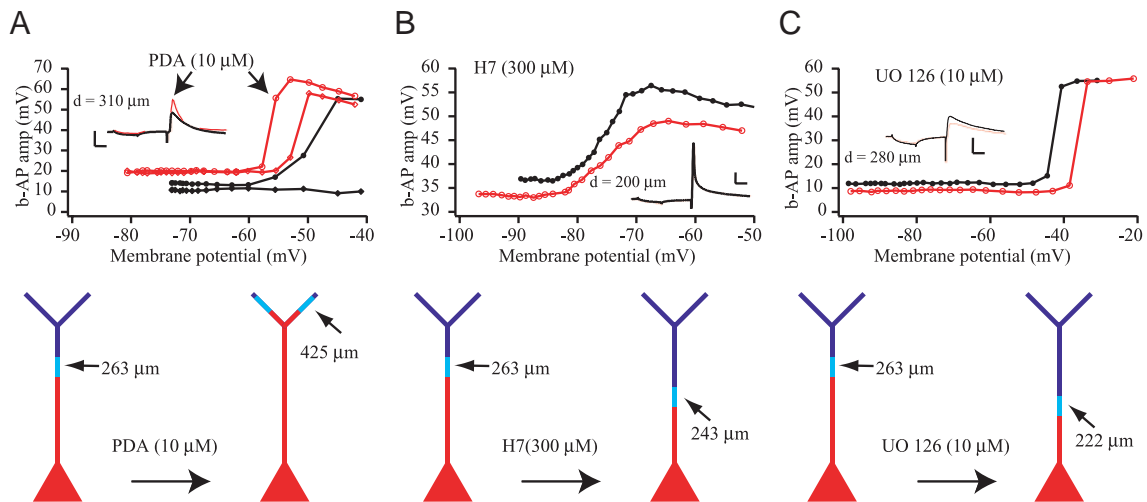


FIG. 8. Modification of  $\theta$  after phosphorylation and dephosphorylation processes. *A*: application of the protein kinase C (PKC) activator PDA ( $10 \mu\text{M}$ ) shifted the transition threshold to a more negative value. Example of a dendrite recorded  $310 \mu\text{m}$  from the soma. *Top*: variation of b-AP amplitude as a function of membrane potential before (filled black circles) and after PDA (empty red circles) for the first b-AP in a train as in Fig. 7.  $\text{Amp}(V_m)$  and  $\theta$  were shifted to the left after PKC activation. The amplitude of the 1st b-AP was larger at all membrane potentials. *Inset*: b-AP before (black) and after (red) PDA at RMP ( $-72 \text{ mV}$ ). Scale bar:  $10 \text{ mV}/10 \text{ ms}$ . Filled black diamonds and empty red diamonds represent the variation of the amplitude of the 5th b-AP in the train before and after PDA, respectively. Note that the amplitude of the 5th b-AP remained constant at all membrane potentials as  $\theta_{5\text{th}}$  was not reached in this example. After PDA,  $\theta_{5\text{th}}$  was shifted toward more negative values within the range of variation of membrane potential tested. *Bottom*: the shift to the right of  $\theta_{1\text{st}}$  resulted in a shift toward the distal part of the dendritic tree of the portion of the apical dendrite that had b-APs with a large amplitude, from  $263$  to  $425 \mu\text{m}$ . *B*: application of the broad spectrum protein kinase inhibitor H7 ( $300 \mu\text{M}$ ) shifted the transition threshold to a more positive value. Example of a dendrite recorded  $200 \mu\text{m}$  from the soma. *Top*: variation of b-AP amplitude as a function of membrane potential before (filled black circles) and after H7 (empty red circles).  $\text{Amp}(V_m)$  and  $\theta$  were shifted to the right. The amplitude of b-APs was decreased at all membrane potentials after H7, showing that the endogenous phosphorylation of  $\text{Na}^+$  and  $\text{K}^+$  channels increased the amplitude of b-APs. The minimum and maximum amplitudes of b-APs were both decreased after H7. *Inset*: b-AP before (black) and after (red) 4-AP at RMP ( $-61 \text{ mV}$ ). Traces were superimposed, because the decrease in b-AP amplitude after H7 was not visible at this scale. Scale bar:  $10 \text{ mV}/10 \text{ ms}$ . *Bottom*: the shift to the right of  $\theta$  resulted in a shift toward a more proximal portion of the apical dendrite that had b-APs with a large amplitude, from  $263$  to  $243 \mu\text{m}$ . *C*: application of the MEK inhibitor U0126 ( $10 \mu\text{M}$ ) shifted the transition threshold to a more positive value. Example of a dendrite recorded  $280 \mu\text{m}$  from the soma. *Top*: variation of b-AP amplitude as a function of membrane potential before (filled black circles) and after U0126 (empty red circles). *Inset*: b-AP before (black) and after (red) U0126 at RMP ( $-63 \text{ mV}$ ). Scale bar:  $10 \text{ mV}/10 \text{ ms}$ . *Bottom*: the shift to the right of  $\theta$  resulted in a shift toward a more proximal portion of the apical dendrite that had b-APs with a large amplitude, from  $263$  to  $222 \mu\text{m}$ .

$\text{Na}^+/\text{K}^+$  channels availability changes  $\theta_x$ , in particular the dendritic region where  $\theta_x = \text{RMP}$ , and thus the degree of penetration of the dendritic tree by large b-APs. This allows us to propose a general framework for back-propagation.

### Back-propagation in dendrites

The state of the membrane potential and back-propagating action potentials are in constant interaction. On the one hand, the amplitude of a b-AP at any dendritic location depends on the availability of ionic channels at this location, such as the density of  $\text{Na}^+$  and  $\text{K}^+$  channels, their activation state (open, inactivated, closed), and their phosphorylation level. On the other hand, a b-AP activates voltage-gated  $\text{Na}^+$ ,  $\text{K}^+$ , and  $\text{Ca}^{2+}$  channels. The state of the membrane is changed thereafter as some of these channels may remain inactivated, or as  $\text{Ca}^{2+}$  entry may in turn activate  $\text{Ca}^{2+}$ -dependent channels and trigger various intracellular second messengers. Therefore b-APs can modify subsequent events including later b-APs, synaptic inputs, and synaptic plasticity. The manner in which a b-AP modifies the state of the membrane at a given dendritic location depends on several parameters that characterize the b-AP, including its rise time, decay phase, and amplitude. We have focused on the amplitude of the b-AP because of the direct relationship between the potential reached by the membrane at

the peak of the b-AP and the opening of the various voltage-gated channels. The availability of voltage-gated channels in dendrites depends on their density, their state of activation/inactivation, and their voltage ranges for activation/inactivation. Opening, inactivation, de-inactivation, and closing of ionic channels are all voltage-dependent processes. A change of membrane potential will thus modify the respective ratio of open/inactivated/closed channels (Pan and Colbert 2001). Previous studies have reported that small-amplitude b-APs can be boosted when appropriately timed with membrane depolarization and that the amplitude of large b-APs could be decreased after membrane hyperpolarization (Magee and Johnston 1997; Stuart and Hausser 2001; Tsubokawa and Ross 1996). Here, we have characterized the membrane potential dependence of b-AP amplitude. We report that if the membrane potential at a given dendritic location is lower than  $\theta_x$ , the amplitude of the b-AP is small and roughly constant across the range of potentials more negative than  $\theta_x$ . We suggest that these b-APs correspond to a mostly passive back-propagation because the  $\text{Na}^+$  channel blocker TTX does not affect their amplitude. In contrast, the amplitude of the b-AP becomes larger as the difference between membrane potential and  $\theta_x$  increases. We suggest that when  $V_m$  becomes larger than  $\theta_x$ , the active component of back-propagation becomes predominant be-

cause the amplitude of the b-AP becomes TTX-sensitive. The value of  $\theta_x$  determines at which membrane potential the amplification of b-APs starts to occur in the distal part of the dendritic tree when b-APs and excitatory postsynaptic potentials (EPSPs) or membrane oscillations are appropriately timed (Johnston et al. 2000; Magee and Johnston 1997; Stuart and Hausser 2001).

A transition threshold was found in 62 of 65 dendritic recordings. Pyramidal neurons with split dendrites at a distance  $>260 \mu\text{m}$  from the soma had a transition threshold regardless of which dendritic branch was recorded (the recording site was identified morphologically). In three instances ( $>300 \mu\text{m}$  from the soma), membrane depolarization evoked an action potential before the arrival of the b-AP, and the transition threshold could not be measured. These recordings were not the most distal ones from our database.

We have found that the rising phase of the curve giving the amplitude of b-APs as a function of  $V_m$  (duration of the transition zone) was variable even for dendritic recordings performed at similar distances from the soma, from step-like to smooth sigmoid-like functions. The parameters controlling the duration of the transition remain to be investigated. Small variations of membrane potential around  $\theta_x$  can produce a jitter of b-AP amplitude that depends on the length of the transition zone.

Theta is a meta-parameter that takes into account the state of ionic channels. Because voltage-gated channels interact with each other, it is very difficult to establish the exact contribution of one type of channel to a b-AP. Not surprisingly, because back-propagation is primarily controlled by  $\text{Na}^+$  and  $\text{K}^+$  channels, a modification of their availability modifies  $\theta$ . This was demonstrated using a variety of approaches including a decrease in the number of channels (via their partial blockade), their inactivation (via repetitive stimulation), and a change in their activation curve (via phosphorylation-dephosphorylation). It is tempting to correlate the linear increase of  $\theta_x$  with the linear increase of A type of  $\text{K}^+$  channels as a function of the distance from the soma (Hoffman et al. 1997). However, because the distribution and properties of the various types of  $\text{Ca}^{2+}$  channels also vary along the dendritic tree (Magee et al. 1998), the contribution of these channels to  $\theta$  remains to be investigated.

The existence of a location-dependent transition threshold in the dendrites means that at a given distance  $\theta_x = \text{RMP}$ . We have found a value of  $x = 260 \mu\text{m}$ , suggesting that at this distance there is a transition from predominantly active to predominantly passive back-propagation at RMP. This cut-off distance is very close to the  $280 \mu\text{m}$  value found in vivo above which b-APs have a small amplitude (Kamondi et al. 1998a). The dispersion of b-AP amplitudes between  $200$  and  $260 \mu\text{m}$  in Fig. 1 is consistent with the jitter of amplitude expected to occur in this dendritic region. The dispersion may reflect the fact that the state of ionic channel may be different from one cell to another at similar recording locations, e.g., different phosphorylation levels. Therefore in CA1 pyramidal cell dendrites, b-APs decrease in amplitude as they travel away from the soma under a combination of factors including dendritic morphology (Vetter et al. 2001), the increase of A-type  $\text{K}^+$  channels (Hoffman et al. 1997), and the value of  $\theta_x$  at any dendritic location (present study). The large variability of amplitudes recorded in distal dendrites previously reported

(Golding et al. 2001; Johnston and Spruston 1992; Magee and Johnston 1995; Tsubokawa and Ross 1996) may stem from the difference between RMP and  $\theta_x$  in each experimental condition.

#### *Functional consequences*

In vivo recordings indicate that membrane potential can fluctuate between  $-80$  and  $-40$  mV (Kamondi et al. 1998a,b). Because most values of  $\theta$  (90%) are bounded by these two potentials, switching between weak and strong back-propagation is physiologically relevant. A stronger depolarization is required as the distance with the soma increases for the transition to occur. This condition can be met by appropriately timed EPSPs and b-APs because the increase in amplitude of dendritic EPSPs with the distance from the soma (Magee and Cook 2000) could compensate for the decremental back-propagation. This would constitute another normalization process in the dendrites (Magee 1999; Magee and Cook 2000). We have also observed the switch from large- to small-amplitude b-APs in more proximal parts of the dendritic tree using membrane potential oscillation or hyperpolarization. The functional consequences for limiting the invasion of the dendritic tree by b-APs remain to be investigated.

Numerous hippocampal functions are associated with rhythmic oscillations at various frequencies (Freund and Buzsáki 1996) for which dendrites may play an important role (Kamondi et al. 1998b; Magee 2001). b-AP timing in the oscillation and the frequency of the latter will determine the degree of invasion of the dendritic tree because close to the trough or the peak of the oscillation, b-APs will have a small or a large amplitude, respectively.

Repetitive firing is also part of the cell repertoire found in vivo. The progressive inactivation of  $\text{Na}^+$  channels makes each b-AP have its own  $\theta$  value. This defines a window of membrane potential inside which only the first of two consecutive b-APs has a large amplitude. Outside this window, the amplitude of both b-APs is either small or large. This window may be important for temporal coding in dendrites (Williams and Stuart 2000).

The other important characteristic of  $\theta$  is its plasticity. Many physiological factors can change the availability of ionic channels. This includes a change in their number (internalization/insertion) or of their activation/inactivation/de-inactivation curves via their numerous modulatory sites. For example, their phosphorylation or dephosphorylation, which can occur in many physiological (synaptic plasticity) and pathological (epilepsy and ischemia) conditions, will modify these curves and thus  $\theta$ . A change in  $\theta$  is likely to alter information processing in the dendrites.

All these arguments emphasize the importance of understanding the dynamic character of back-propagation. Given the high rate of spontaneous excitatory activity received by pyramidal cells in vivo in certain conditions (Pare et al. 1997), large-amplitude b-APs may invade extensively the dendritic tree. Conversely, GABAergic activity-dependent oscillations (Buzsáki 2002) may limit this invasion (Tsubokawa and Ross 1996), although this will be dependent on the depolarizing or hyperpolarizing action of GABA in the dendrites (Gulledge and Stuart 2003). Finally, during high-frequency firing, the long recovery rate from inactivation of  $\text{Na}^+$  channels (Colbert

et al. 1997) is an efficient way to limit the invasion and thus the triggering of Ca-dependent modifications.

In conclusion, the existence of state-dependent and modifiable transition threshold endows the cell with the ability to dynamically fine tune the degree of invasion of the dendritic tree by b-APs and thus the amount of depolarization and  $\text{Ca}^{2+}$  entry. The transition threshold may be both a useful parameter for characterizing a dendritic tree as well as a critical parameter for dendritic information processing.

We thank Dr. Rick Gray for computer help, and Drs. Costa Colbert and Nick Poolos for their helpful comments on the manuscripts. CB also thanks Dr. Yong Liang and other members of the lab for help with animal dissections.

#### DISCLOSURES

This work was supported by Institut National de la Santé Et de la Recherche Médicale, National Institutes of Health Grants NS-37444, MH-44754, and MH-48432, Ligue Française Contre l'Epilepsie-SANOFI, and the Philippe Foundation.

#### REFERENCES

- Adams JP and Sweatt JD.** Molecular psychology: roles for the ERK MAP kinase cascade in memory. *Annu Rev Pharmacol Toxicol* 42: 135–163, 2002.
- Buzsáki G.** Theta oscillations in the hippocampus. *Neuron* 33: 325–340, 2002.
- Callaway JC and Ross WN.** Frequency-dependent propagation of sodium action potentials in dendrites of hippocampal CA1 pyramidal neurons. *J Neurophysiol* 74: 1395–1403, 1995.
- Colbert CM and Johnston D.** Axonal action-potential initiation and  $\text{Na}^+$  channel densities in the soma and axon initial segment of subicular pyramidal neurons. *J Neurosci* 16: 6676–6686, 1996.
- Colbert CM and Johnston D.** Protein kinase C activation decreases activity-dependent attenuation of dendritic  $\text{Na}^+$  current in hippocampal CA1 pyramidal neurons. *J Neurophysiol* 79: 491–495, 1998.
- Colbert CM, Magee JC, Hoffman DA, and Johnston D.** Slow recovery from inactivation of  $\text{Na}^+$  channels underlies the activity-dependent attenuation of dendritic action potentials in hippocampal CA1 pyramidal neurons. *J Neurosci* 17: 6512–6521, 1997.
- Cossart R, Hirsch JC, Cannon RC, Dinocourt C, Wheal HV, Ben Ari Y, Esclapez M, and Bernard C.** Distribution of spontaneous currents along the somato-dendritic axis of rat hippocampal CA1 pyramidal neurons. *Neuroscience* 99: 593–603, 2000.
- Durand D, Carlen PL, Gurevich N, Ho A, and Kunov H.** Electrotonic parameters of rat dentate granule cells measured using short current pulses and HRP staining. *J Neurophysiol* 50: 1080–1097, 1983.
- English JD and Sweatt JD.** Activation of p42 mitogen-activated protein kinase in hippocampal long-term potentiation. *J Biol Chem* 271: 24329–24332, 1996.
- Freund TF and Buzsáki G.** Interneurons of the hippocampus. *Hippocampus* 6: 347–470, 1996.
- Gasparini S and Magee JC.** Phosphorylation-dependent differences in the activation properties of distal and proximal dendritic  $\text{Na}^+$  channels in rat CA1 hippocampal neurons. *J Physiol* 541: 665–672, 2002.
- Golding NL, Kath WL, and Spruston N.** Dichotomy of action-potential backpropagation in CA1 pyramidal neuron dendrites. *J Neurophysiol* 86: 2998–3010, 2001.
- Gulledge AT and Stuart GJ.** Excitatory actions of GABA in the cortex. *Neuron* 37: 299–309, 2003.
- Hoffman DA and Johnston D.** Downregulation of transient  $\text{K}^+$  channels in dendrites of hippocampal CA1 pyramidal neurons by activation of PKA and PKC. *J Neurosci* 18: 3521–3528, 1998.
- Hoffman DA and Johnston D.** Neuromodulation of dendritic action potentials. *J Neurophysiol* 81: 408–411, 1999.
- Hoffman DA, Magee JC, Colbert CM, and Johnston D.**  $\text{K}^+$  channel regulation of signal propagation in dendrites of hippocampal pyramidal neurons. *Nature* 387: 869–875, 1997.
- Johnston D, Hoffman DA, Colbert CM, and Magee JC.** Regulation of back-propagating action potentials in hippocampal neurons. *Curr Opin Neurobiol* 9: 288–292, 1999.
- Johnston D, Hoffman DA, Magee JC, Poolos NP, Watanabe S, Colbert CM, and Migliore M.** Dendritic potassium channels in hippocampal pyramidal neurons. *J Physiol* 525: 75–81, 2000.
- Johnston D and Spruston N.** Perforated patch-clamp analysis of the passive membrane properties of three classes of hippocampal neurons. *J Neurosci* 67: 508–529, 1992.
- Kamondi A, Acsády L, and Buzsáki G.** Dendritic spikes are enhanced by cooperative network activity in the intact hippocampus. *J Neurosci* 18: 3919–3928, 1998a.
- Kamondi A, Acsády L, Wang XJ, and Buzsáki G.** Theta oscillations in somata and dendrites of hippocampal pyramidal cells in vivo: activity-dependent phase-precession of action potentials. *Hippocampus* 8: 244–261, 1998b.
- Magee JC.** Dendritic hyperpolarization-activated currents modify the integrative properties of hippocampal CA1 pyramidal neurons. *J Neurosci* 18: 7613–7624, 1998.
- Magee JC.** Dendritic  $I_h$  normalizes temporal summation in hippocampal CA1 neurons. *Nat Neurosci* 2: 508–514, 1999.
- Magee JC.** Dendritic mechanisms of phase precession in hippocampal CA1 pyramidal neurons. *J Neurophysiol* 86: 528–532, 2001.
- Magee JC and Cook EP.** Somatic EPSP amplitude is independent of synapse location in hippocampal pyramidal neurons. *Nat Neurosci* 3: 895–903, 2000.
- Magee J, Hoffman D, Colbert C, and Johnston D.** Electrical and calcium signaling in dendrites of hippocampal pyramidal neurons. *Annu Rev Physiol* 60: 327–346, 1998.
- Magee JC and Johnston D.** Synaptic activation of voltage-gated channels in the dendrites of hippocampal pyramidal neurons. *Science* 268: 301–304, 1995.
- Magee JC and Johnston D.** A synaptically controlled, associative signal for Hebbian plasticity in hippocampal neurons. *Science* 275: 209–213, 1997.
- Martina M, Vida I, and Jonas P.** Distal initiation and active propagation of action potentials in interneuron dendrites. *Science* 287: 295–300, 2000.
- Pan E and Colbert CM.** Subthreshold inactivation of  $\text{Na}^+$  and  $\text{K}^+$  channels supports activity-dependent enhancement of back-propagating action potentials in hippocampal CA1. *J Neurophysiol* 85: 1013–1016, 2001.
- Pare D, Lebel E, and Lang EJ.** Differential impact of miniature synaptic potentials on the soma and dendrites of pyramidal neurons in vivo. *J Neurophysiol* 78: 1735–1739, 1997.
- Quirk MC, Blum KI, and Wilson MA.** Experience-dependent changes in extracellular spike amplitude may reflect regulation of dendritic action potential back-propagation in rat hippocampal pyramidal cells. *J Neurosci* 21: 240–248, 2001.
- Spruston N, Schiller Y, Stuart G, and Sakmann B.** Activity-dependent action potential invasion and calcium influx into hippocampal CA1 dendrites. *Science* 268: 297–300, 1995.
- Stuart G and Hausser M.** Initiation and spread of sodium action potentials in cerebellar Purkinje cells. *Neuron* 13: 703–712, 1994.
- Stuart GJ and Hausser M.** Dendritic coincidence detection of EPSPs and action potentials. *Nat Neurosci* 4: 63–71, 2001.
- Stuart G, Spruston N, Sakmann B, and Hausser M.** Action potential initiation and backpropagation in neurons of the mammalian CNS. *Trends Neurosci* 20: 125–131, 1997.
- Tsubokawa H and Ross WN.** IPSPs modulate spike backpropagation and associated  $[\text{Ca}^{2+}]_i$  changes in the dendrites of hippocampal CA1 pyramidal neurons. *J Neurophysiol* 76: 2896–2906, 1996.
- Vetter P, Roth A, and Hausser M.** Propagation of action potentials in dendrites depends on dendritic morphology. *J Neurophysiol* 85: 926–937, 2001.
- Watanabe S, Hoffman DA, Migliore M, and Johnston D.** Dendritic  $\text{K}^+$  channels contribute to spike-timing dependent long-term potentiation in hippocampal pyramidal neurons. *Proc Natl Acad Sci USA* 99: 8366–8371, 2002.
- Williams SR and Stuart GJ.** Backpropagation of physiological spike trains in neocortical pyramidal neurons: implications for temporal coding in dendrites. *J Neurosci* 20: 8238–8246, 2000.
- Yuan LL, Adams JP, Swank M, Sweatt JD, and Johnston D.** Protein kinase modulation of dendritic  $\text{K}^+$  channels in hippocampus involves a mitogen-activated protein kinase pathway. *J Neurosci* 22: 4860–4868, 2002.